The importance of agostic-type interactions for the binding energies of Ni^+ to saturated and α,β-unsaturated alkanes, silanes and germanes

Inés Corral, Otilia Mó and Manuel Yáñez*

Departamento de Química, C-9, Universidad Autónoma de Madrid, Cantoblanco, 28049, Madrid, Spain. E-mail: manuel.yanez@uam.es

Received (in Montpellier, France) 15th May 2003, Accepted 24th June 2003
First published as an Advance Article on the web 4th September 2003

The gas-phase interaction of $H_3C–CH_2–XH_3$ and $H_2C{=}C(H)XH_3$ (X = C, Si, Ge) with Ni^+ has been investigated through the use of high-level density functional theory methods. The structures of the corresponding Ni^+ complexes were optimized at the B3LYP/6-311G(d,p) level of theory. Final energies were obtained in single-point B3LYP/6-311+G(2df,2p) calculations. In all cases, the most stable complexes are stabilized through agostic-type interactions between the metal cation and the hydrogen atoms of the XH_3 group. Only for propene is the conventional π-complex the global minimum of the potential energy surface. These agostic-type linkages can be viewed as three-center bonds resulting from electron-donor interactions between σ bonding orbitals of the neutral and the empty s orbital of the metal and back-donation from pairs of valence electrons of the metal into the corresponding σ* antibonding orbitals of the neutral. As a consequence, these bonds are particularly stable for Si- and Ge-containing compounds, because of the high electron-donor ability of the XH_3 group when the heteroatom is Si or Ge. Vinylsilane and vinylgermane lead to non-conventional complexes in which the metal bridges the C_α atom of the C=C double bond and one of the hydrogen atoms of the XH_3 group. In contrast with the behavior predicted when the reference acid is Cu^+, Si- and Ge-derivatives, both saturated and unsaturated, bind Ni^+ more strongly than propane and propene, respectively. Ni^+ binding energies are systematically greater than Cu^+ binding energies and the bond activation effects observed upon Ni^+ attachment are sizably larger than those found upon Cu^+ association.

Introduction

Many relevant processes in chemistry and biochemistry involve interactions with transition metal cations. This has motivated a considerable interest in the study of the gas-phase reactions between organic and inorganic compounds with transition metal monocations.[1–10] In spite of this, the number of accurate cation metal binding energies is still scarce[11] and much of this information was obtained by means of *ab initio* or density functional theory (DFT) calculations.[11] The situation is even worse when dealing with compounds that present second- and third-row atoms as active centers.

In our group we have devoted some efforts to investigating the intrinsic reactivity of organic bases containing second-, third- and fourth-row basic centers with the aim of establishing reactivity trends with respect to different reference acids.[12–23] These analyses allowed us to conclude that, very often, there is a dramatic change in the reactivity patterns when a first-row basic center is replaced by a second-row or a third-row one. Phosphines and arsines are suitable examples of compounds that exhibit a behavior markedly different from that observed for the corresponding amines.[12] Another interesting set is that represented by silanes and germanes in contraposition to the corresponding alkanes. Also in this case the reactivity of silanes and germanes in protonation and/or deprotonation processes might be very different from that exhibited by the corresponding carbon-containing analogs.

This is the case, for instance, for α,β-unsaturated silanes and germanes.[18–20,23,24] Not much is known about the chemistry of these species because they have been synthesized for the first time only a few years ago and because some of them are not very stable.[25,26] The experimental determination of their intrinsic acidities and a theoretical estimate of their intrinsic basicities were reported recently in the literature[18,23] and show significant dissimilarities between C- and Si- or Ge-containing compounds. Later on we have also shown[19,20] that the reactivity of these compounds toward Cu^+ presents important peculiarities. Even though the Cu^+ complexes very often closely resemble the corresponding protonated species due to the non-negligible covalent character of the neutral–Cu^+ interactions,[17,27–30] this is not the case for silanes and germanes, for which agostic-type interactions between the transition metal cation and the hydrogen atoms of the XH_3 (X = Si, Ge) moiety are extremely strong,[19,20,24] leading to an enhancement of the basicity of these systems with respect to that of the corresponding hydrocarbons, for which the interactions between Cu^+ and the CH_3 group are much weaker.

The aim of this paper is to extend this study to complexes with Ni^+, that unlike Cu^+, is an open-shell cation. The questions we want to address are whether similar agostic-type bonds are formed when the reference acid is Ni^+ and whether these interactions are stronger or weaker than those obtained when the reference acid is Cu^+. This would also permit us to investigate whether or not the reactivity trends along the group 14 elements with respect to these two transition metal cations are similar or different, for both saturated and unsaturated compounds.

Computational details

The B3LYP density functional theory approach, combined with a 6-311+G(2df,2p) basis set, has been proved to be very

DOI: 10.1039/b305532a

well-suited for the description of Cu^+ and Ni^+ complexes and to obtain Cu^+ and Ni^+ binding energies in fairly good agreement with the experimental values.[31,32] In some cases this approach has been found to be superior to the most commonly used *ab initio* approaches due to frequent instabilities of the HF wavefunction and to poor convergency of the MPn series[31,33,34] that render these single-reference *ab initio* methods less reliable. The B3LYP method, as implemented in the Gaussian-98 series of programs,[35] combines Becke's three-parameter nonlocal hybrid exchange potential[36] with the non-local correlation functional of Lee, Yang and Parr.[37] In our theoretical model the single point B3LYP/6-311+G(2df,2p) calculations were carried out on B3LYP/6-311G(d,p) optimized geometries. The harmonic vibrational frequencies were obtained also at the B3LYP/6-311G(d,p) level in order to assess that the stationary points found in our survey of the potential energy surface (PES) correspond to local minima and to estimate the corresponding zero point energy (ZPE) corrections. The 6-311+G(2df,2p) basis set for Ni^+ corresponds to the (14s9p5d/9s5p3d) basis set expansion of Watchers[38] and Hay,[39] supplemented with a set of (1s2p1d) diffuse functions and with two sets of f functions and one set of g functions. In all cases the $\langle S^2 \rangle$ expectation value was close to the exact value for a doublet state (see Table 1), indicating that the spin contamination of our unrestricted calculations was reasonably small.

Table 1 Total energies (E), S^2 expectation values ($\langle S^2 \rangle$), zero point energies (ZPE) and Ni^+ binding energies (D_0) of $CH_3CH_2XH_3$ and $H_2C{=}CHXH_3$ (X = C, Si, Ge) compounds and their Ni^+ complexes

	E^a /hartree	$\langle S^2 \rangle$	ZPE^b / hartree	$D_0{}^c$ / kJ mol^{-1}
CH_3	−39.8578097	0.753	0.0290	–
CH_3–Ni^+	−1547.8855986	2.004	0.0341	163.6
Propane	−119.1884727		0.1009	–
S–C1	−1627.2037730	0.764	0.1014	143.2 (118.4)^d
S–C2	−1627.1883634	0.788	0.1008	104.2
S–C3	−1627.1950078	0.783	0.1009	121.4
Ethylsilane	−370.5826021		0.0880	–
S–Si1	−1878.6106826	0.754	0.0894	174.3
S–Si2	−1878.5903214	0.783	0.0871	126.8
S–Si3	−1878.5816723	0.785	0.0879	102.0
S–Si4	−1878.6203777	0.757	0.0891	200.2 (170.7)^d
Ethylgermane	−2158.0653597		0.0864	–
S–Ge1	−3666.0958984	0.754	0.0871	182.4
S–Ge2	−3666.0694019	0.775	0.0859	116.0
S–Ge3	−3666.0652331	0.785	0.0861	104.5
S–Ge4	−3666.1046354	0.757	0.0865	206.9 (179.5)^d
Propene	−117.9535866		0.0777	–
U–C1	−1625.9963154	0.761	0.0804	209.3 (200.0)^d
U–C2	−1625.9547748	0.778	0.0779	106.8
Vinylsilane	−369.3465658		0.0654	–
U–Si1	−1877.3852236	0.762	0.0673	200.6
U–Si2	−1877.3695584	0.755	0.0660	162.9
U–Si3	−1877.3963555	0.759	0.0678	228.7 (192.5)^d
Vinylgermane	−2156.8281731		0.0636	–
U–Ge1	−3664.8665146	0.762	0.0655	199.9
U–Ge2	−3664.8654218	0.757	0.0639	201.2
U–Ge3	−3664.8797145	0.759	0.0657	234.1 (199.2)^d

[a] Calculated at the B3LYP/6-311+G(2df,2p) level. [b] Calculated at the B3LYP/6-311G(d,p) level. [c] Calculated at the B3LYP/6-311+G(2df,2p) level including ZPE corrections (see text). [d] Cu^+ binding energies taken from ref. 19.

The corresponding Ni^+ binding energies, D_0, were evaluated by subtracting from the energy of the complex the energy of the neutral and that of Ni^+, after including the corresponding zero point energy (ZPE) corrections, which were scaled by the empirical factor 0.98.[40]

Unfortunately, there are not many experimental Ni^+ binding energies involving hydrocarbons accurate enough as to be used as a reference to assess the reliability of our theoretical method.[11] As a matter of fact, we are only aware of the different values reported by Georgiadis *et al.*[41] for the Ni^+–CH_3 binding energies. Hence, we have used this molecule to test our model. The value obtained for the corresponding Ni^+ binding enthalpy, after including the corresponding thermal corrections and the PV term, is 169 kJ mol^{-1}, which lies within the error limits of the different experimental estimates (174.9 ± 15.5 and 188.3 ± 10.0 kJ mol^{-1}) reported in ref. [41], and which is in fairly good agreement with previous theoretical estimates reported by Bauschlicher *et al.*[42] using different theoretical schemes.

The atoms in molecules (AIM) theory of Bader[43] was used to investigate the bonding characteristics of the different Ni^+ complexes investigated and, in particular, the possible bond activations undergone by the neutral upon Ni^+ association and to characterize the possible agostic-type linkages arising from these interactions. The AIM theory is based in a topological analysis of the electron charge density, $\rho(r)$ and its Laplacian, $\nabla^2\rho(r)$. More specifically, we have located the so-called bond critical points (bcps), that is the points where $\rho(r)$ is a minimum along the bond path and a maximum in the other two directions. In general the values of ρ and $\nabla^2\rho$ at these points provide useful information on the bonding characteristics. In most cases negative values of the Laplacian are associated with covalent linkages, while positive values are usually associated with closed-shell interactions such as those found in ionic bonds, van der Waals complexes and hydrogen bonds. More reliable for this purpose is the energy density, $H(r)$, in the sense that negative values of $H(r)$ are always associated with covalent linkages even in those particular cases, such as the F_2 molecule, where the Laplacian is positive. This analysis will be complemented with that carried out in terms of the lengthening or shortening of the bond lengths and in terms of the shifting of the corresponding stretching frequencies. A second-order perturbation analysis in the framework of the NBO population method[44] will be used to quantitatively characterize the donor-acceptor interactions between occupied (empty) orbitals of the neutral and vacant (occupied) orbitals of Ni^+ that are responsible for the agostic-type interactions that stabilize these complexes.

Results and discussion

Structures, relative stabilities and bonding

The structures of the different saturated $CH_3CH_2XH_3$ and unsaturated $H_2C{=}CHXH_3$ (X = C, Si, Ge) species as well as those of their Ni^+ complexes are given in Fig. 1. Their total energies are summarized in Table 1. Table 1 contains also the calculated binding energies, D_0. In our discussion the numbering showed in Scheme 1 will be systematically used.

Saturated compounds. The structures of Ni^+ complexes closely resemble those described before in the literature for the analogous Cu^+ complexes.[20] More specifically, although the interaction of Ni^+ with the CH_2, CH_3 and XH_3 groups leads to stable structures that are local minima of the corresponding potential energy surface (PES), with propane the global minimum, **S–C1**, corresponds to a complex in which Ni^+ interacts simultaneously with the two terminal CH_3 groups. A similar structure was reported before in the literature for the

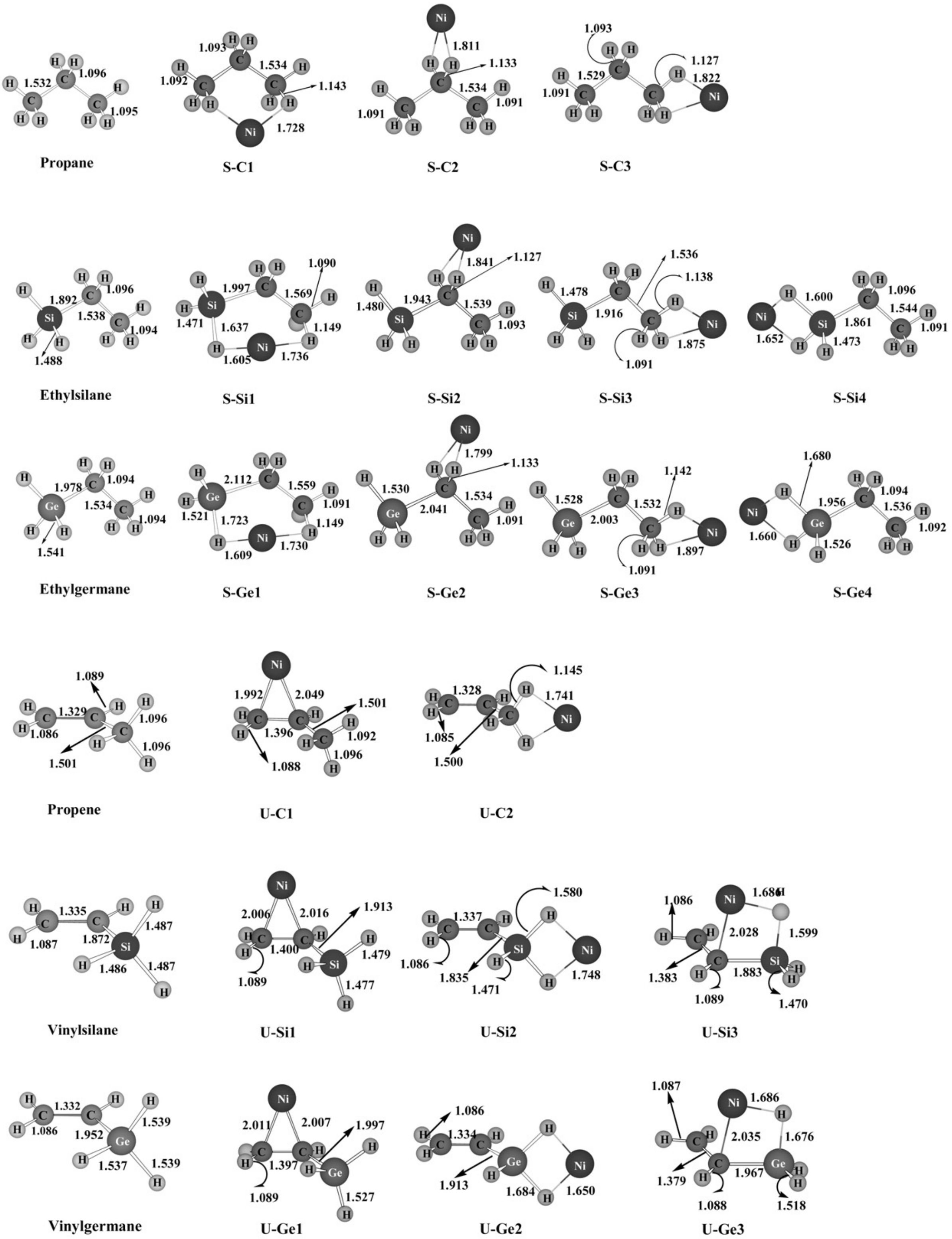

Fig. 1 B3LYP/6-311G(d,p) optimized geometries of $CH_3CH_2XH_3$ and $H_2C{=}CHXH_3$ (X = C, Si, Ge) and their Ni^+ complexes. Bond lengths in Å and bond angles in degrees.

propane–Co^+ complex.[45] The other two local minima, namely **S–C2** and **S–C3**, are predicted to be 39.0 and 21.8 kJ mol^{-1} higher in energy, respectively. It is worth noting that these energy gaps are significantly larger than those calculated for the corresponding Cu^+ complexes. These changes in the energy gaps between the different local minima, when Cu^+ is replaced by Ni^+, point to sizable bonding differences between these metal cations, which will be analyzed later.

Important changes in the intrinsic reactivity of the system are found when one of the terminal methyl groups is replaced by an XH_3 (X = Si, Ge) group. Indeed the structures in which Ni^+ bridges the CH_3 and the XH_3 terminal groups, namely **S–Si1** and **S–Ge1**, are not the global minima of the PES because the interaction of Ni^+ exclusively with the XH_3 group (X = Si, Ge) to yield structures **S–Si4** and **S–Ge4**, is predicted to be about 25 kJ mol^{-1} stronger. Again, the **S–Si4**/**S–Si1** and **S–Ge4**/**S–Ge1** energy gaps are twice as large as those estimated for the corresponding Cu^+-containing analogs. In all cases the attachment of the metal cation to the CH_3 group yields the less stable complexes, namely **S–C3**, **S–Si3**and **S–Ge3**.

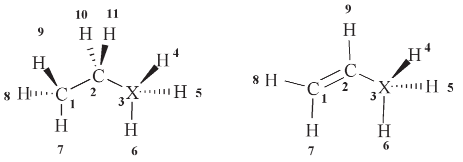

Scheme 1

The strong interaction of Ni^+ with the XH_3 (X = Si, Ge) group of ethylsilane and ethylgermane results in a quite large binding energy, which is more than 57 kJ mol^{-1} higher than that of propane. To understand these differences, let us analyze in some detail the bonding characteristics of these complexes. In Fig. 2 we have plotted the bond paths and the position of the bcps for the more stable Ni^+ complexes. It can be observed that the interaction of Ni^+ with propane to yield complex **S–C1** results in the formation of two Ni–H linkages. The cyclic character of this structure is ratified by the existence of a ring critical point with an electron density of 0.030 e au^{-3}. Concomitantly, the charge density at the bcp of the C–H bonds that interact with Ni^+ (C1–H7 and C3–H6) is significantly smaller than that calculated for the C–H bonds that do not participate in the interaction. Consistently, the bond lengths of these two C–H linkages significantly increase upon Ni^+ association (see Fig. 1) and the corresponding C–H stretching frequencies appear significantly red-shifted and combined as symmetric and antisymmetric modes (see Table 2). A similar topological analysis for **S–Si4** and **S–Ge4** clearly shows that the interactions between Ni^+ and Si–H or Ge–H bonds are much stronger than the interactions between this cation and C–H linkages, as reflected in a larger value of $\rho(r)$ at the Ni–HSi or Ni–HGe bcps. Also, in these two cases the Si-H or Ge–H bonds involved in the interaction considerably lengthen (see Fig. 1) and the corresponding stretching frequencies appear significantly shifted to the red (see Table 2).

It is also important to emphasize that in all cases the value of $\rho(r)$ at the Ni-H bcps is, at least, three times larger than the values typically found in ionic bonds, indicating that the bond has a non-negligible covalent character. This partial covalent character is also mirrored in the sign of the energy density, which in all cases is negative. In both **S–Si4** and **S–Ge4**, a ring critical point associated with the XH_2Ni four-membered ring was located.

The origin of these stabilizing interactions can be traced through the use of an NBO second-order perturbation analysis. An inspection of the second-order interaction energies for **S–C1** reveals the existence of a dative bond from the two C1–H7 and C3–H6 σ bonding orbitals towards the empty s orbital (actually a 94% 4s, 6% 3d hybrid) of Ni, and back-donation from one of the pairs of valence electrons of Ni into the corresponding C–H σ^* antibonding orbitals (see Table 3). The population of these antibonding orbitals (with occupation number 0.04) is responsible for the weakening and lengthening of these bonds. The situation is rather similar as far as the **S–Si4** and **S–Ge4** complexes are concerned, with the only difference being that now the Si–H or Ge–H σ bonding and σ^* antibonding orbitals belong to the XH_3 (X = Si, Ge) group (see Table 3). This orbital picture is not essentially different from that explaining[45] the bonding between Co^+ and H_2 in terms of donation from the $1\sigma_g$ orbital of H_2 towards the empty 4s orbital of Co^+ and back-bonding from an occupied Co^+ d_{yz} orbital to the H_2 antibonding orbital ($1\sigma_u$).

Most importantly, it can be also observed, in agreement with the AIM results discussed above, that both donation and back-donation interactions with **S–Si4** and **S–Ge4** are characterized by second-order orbital interaction energies significantly greater than those calculated for the **S–C1** complex (see Table 3). Two factors are responsible for this enhanced interaction when the heteroatoms are Si or Ge. On the one hand, the hydrogen atoms of the Si–H and Ge–H bonds behave as electron-rich systems[46] because the electronegativity of Si and Ge leads to a strong polarization of σ_{XH} toward the outer (s-type, hydrogen) end of the orbital.[44] As a matter of fact, the NBO net charges ratify the hydride character of the Si–H and Ge–H bonds,[20] while the polarity of the C–H linkages is $C^{\delta-}$–$H^{\delta+}$. Accordingly, the Si–H and Ge–H bonds are much better electron donors than the C–H linkages. On the other hand, and due to the fact that Si and Ge are bulkier and less electronegative than carbon, the X–H σ^* antibonding orbitals are more diffuse and lie lower in energy than the C–H σ^* antibonding orbitals, favoring the back-donation from the electron pairs of the metal. Consistently, the occupation numbers of the X–H σ^* (X = Si, Ge) antibonding orbitals in complexes **S–Si4** and **S–Ge4** (0.08) are twice as large as those of the C–H σ^* antibonding orbitals in species **S–C1**.

It is also worth noting that the aforementioned interactions are not different in nature from the so-called agostic interactions[47–49] observed in many transition metal complexes and which are characterized by unusual low field shifts in the ^{1}H-NMR spectrum,[50] C–H bond lengthening,[51] reduced C–H stretching frequencies,[51] and remarkably short metal-hydrogen distances.[52] For this reason we shall designate the Ni–HX bonds as agostic-type bonds.

The strong back-donation from the d orbitals of the metal into the σ^*_{XH} antibonding orbitals of the base can be alternatively viewed as three-center two-electron bonds,[52] similar to the ones responsible for the bonding in diborane, in many protonated alkanes[53–56] or in the protonated form of P_4.[57] In the Ni^+ complexes involving saturated compounds, as illustrated in Fig. 3, the highest occupied MOs correspond to three-center bonding combinations that involve a d orbital of the metal and the 1s orbitals of the two hydrogen atoms of the X–H group.

Unsaturated compounds. for unsaturated compounds there are also significant dissimilarities between propene and $H_2C{=}CHXH_3$ (X = Si, Ge). As illustrated in Fig. 1, for propene the conventional π-complex, **U–C1**, is the most stable form, while for the Si- and Ge-containing analogs, a non-conventional structure in which the metal binds simultaneously to C2 and to one of the hydrogen atoms of the XH_3 group (**U–Si3**, **U–Ge3**) is predicted to be 28–34 kJ mol^{-1} more stable than the conventional π-complex (**U–Si1**, **U–Ge1**).

The bonding in complexes **U–C1**, **U–Si3** and **U–Ge3** can be understood again in terms of three-center bonds, with the only difference being that, whereas in the **U–C1** complex the d orbital of the metal interacts with the two p orbitals at C1 and C2 (see Fig. 4), in **U–Si3** and **U–Ge3**, the interaction involves a p orbital of C2 and the s orbital of one of the hydrogen atoms of the XH_3 group (see Fig. 4).

Why are complexes **U–Si3** and **U–Ge3** favored with respect to those in which the metal interacts only with the XH_3 group (**U–Si2**, **U–Ge2**), in contrast with what was observed for the saturated compounds? The main reason is that the electron-donor ability of the XH_3(X = Si, Ge) group decreases on going from the saturated to the unsaturated analog, because in the latter compounds this group is attached to a C=C double bond, which is a much more electronegative group than a C–C single bond. Indeed, the NBO analysis shows that the net negative charge of the hydrogen atoms of the XH_3 group, as expected, decrease in absolute value on going from the saturated to the unsaturated compounds. Consequently, the second-order orbital interaction energies calculated for **U–Si2** and **U–Ge2** are smaller than those obtained for **S–Si4** and **S–Ge4** (see Table 3). As an obvious consequence, it can be also observed that the XH_3 group of the saturated compounds binds Ni^+ more strongly than the XH_3 group of the unsaturated ones.

The reason why, for Si- and Ge-containing compounds, complexes **U–Si3** and **U–Ge3** are also favored with respect to

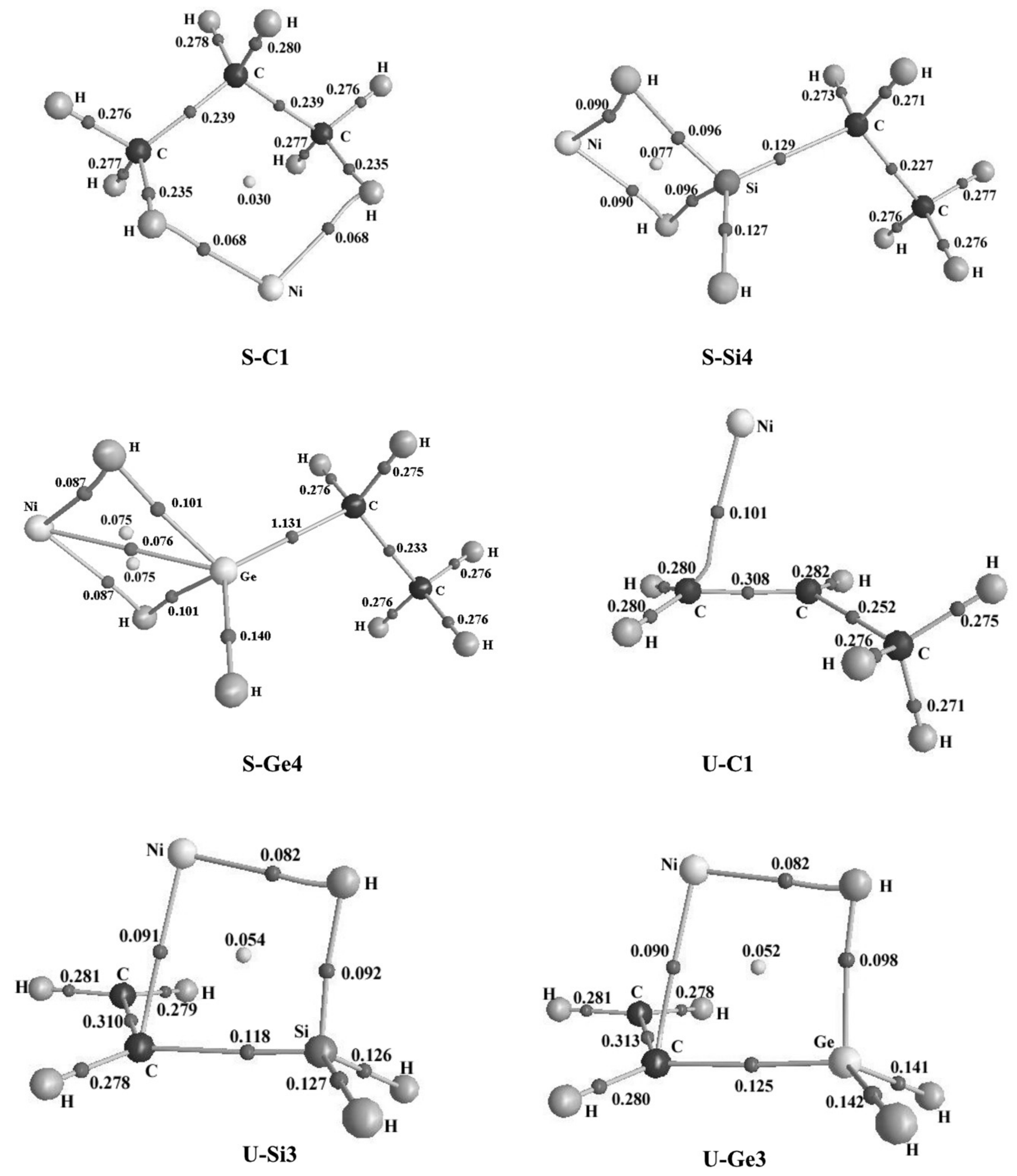

Fig. 2 Molecular graphs of the most stable Ni$^+$ complexes of $CH_3CH_2XH_3$ and $H_2C{=}CHXH_3$ (X = C, Si, Ge) derivatives showing the bond paths, the positions of the bond critical points, ring critical points and the charge density (e au^{-3}) evaluated at these points at the B3LYP/6-311G(d,p) level.

the conventional π-complexes (**U–Si1** and **U–Ge1**) can be understood if one takes into account that, in contrast with what happens in propene, the X–H linkages are better electron donors than C–H bonds, hence the metal tries to interact simultaneously with the two electron-rich groups in the system, the π-cloud and the X–H bonds. From a more quantitative point of view, it can be observed (see Table 3) that, although in complexes **U–Si3** and **U–Ge3** the donation from the C1C2 π bonding orbital into the sd hybrid orbital of Ni is much less stabilizing than in complexes **U–Si1** and **U–Ge1**, the overall stabilization effect is greater due to the contribution of the dative bond from the X–H σ bonding orbital.

These orbital interactions are coherent with the existence of a bond path between Ni and C2 and between Ni and one of the hydrogen atoms of the XH_3 group, as well as with the existence of a ring critical point inside the corresponding four-membered ring (see Fig. 2).

It can be also observed that the back-donation from the electron pairs of the metal to the C1C2 π* antibonding orbital is quantitatively smaller (see Table 3) in **U–Si3** and **U–Ge3** than in **U–Si1** and **U–Ge1** complexes. Consistently, the lengthening of the C1–C2 bond is smaller in the former case (see Fig. 1). For **U–Si3** and **U–Ge3** this back-donation is reflected in a significant red-shifting of the C1=C2 stretching frequency, while

Table 2 Harmonic vibrational frequencies (cm^{-1}) of $CH_3CH_2XH_3$ and $H_2C{=}CHXH_3$ (X = C, Si, Ge) compounds and their most stable Ni^+ complexes

	$CH_3CH_2XH_3$					
Assignment	X = C	**S–C1**	X = Si	**S–Si4**	X = Ge	**S–Ge4**
CH_3 stretch	3084, 3081, 3018	3119,[a] 3112,[a] 3102[a]	3087, 3080, 3022	3116, 3112, 3043	3091, 3075, 3019	3120,[a] 3109,[a] 3100[a]
CH_2 stretch	3034, 3014	3066,[a] 3066[a]	3052, 3019	3080, 3031	3034, 3067	3054,[a] 3041[a]
XH_3 stretch	3083, 3071, 3015	3064,[a] 2537,[b] 2518[b]	2217, 2213, 2212	2298, 1723,[b] 1371[b]	2129, 2125, 2122	2184, 1613,[b] 1537[b]
C–C stretch	871,[c] 1057[d]	869,[c] 1044[d]	982	970	980	968
C–X stretch			597	668	514	567

	$H_2C{=}CHXH_3$					
Assignment	X = C	**U–C1**	X = Si	**U–Si3**	X = Ge	**U–Ge3**
XH_3 stretch	3092, 3056, 3013	3112,[a] 3086, 3028	2226, 2214, 2218	2331, 2295, 1634[b]	2134, 2127, 2128	2228, 2197, 1491[b]
CH_2 stretch (asym.)	3208	3198	3187	3189	3186	3187
CH_2 stretch (sym.) CH stretch	3127, 3120	3105, 3128[a]	3115, 3105	3099, 3129	3126, 3106	3099, 3140
C=C stretch	1712	1553	1656	1545	1656	1374
C–X stretch	924	904	618	697	527	613

[a] Vibrational modes strongly coupled. [b] Stretching of the X–H bond involved in the agostic interaction. [c] CCC symmetric stretch. [d] CCC asymmetric stretch.

only one of the X–H stretching modes appears significantly shifted to low frequency values upon Ni^+ attachment.

It is also interesting to note that the Ni^+ binding energy for propene is predicted to be 19–25 kJ mol^{-1} lower than that of vinylsilane or vinylgermane, in contrast with what was found[20] for Cu^+.

Ni^+ association *vs.* Cu^+ attachment

A comparison between the Ni^+ binding energies reported in this paper and the Cu^+ binding energies given in ref. 20(see Table 1), clearly shows that $H_3C–CH_2–XH_3$ and $H_2C{=}C(H)$-XH_3 (X = C, Si, Ge) compounds bind Ni^+ more strongly than Cu^+. These energetics are also consistent with the quantitative differences observed in the bonding when Cu^+ is replaced by Ni^+. Systematically, the values of $\rho(r)$ at the Ni–H bcps in complexes **S–Si4** and **S–Ge4**, for instance, are systematically larger (0.090 and 0.087 e au^{-3}, respectively) than those obtained[20] for the corresponding Cu–H linkages (0.081 and 0.079 e au^{-3}, respectively). Also, the lengthening of these bonds is greater upon Ni^+ attachment than upon Cu^+ association. For example, on going from ethylsilane to complex **S–Si4**, the Si–H linkages interacting with the metal lengthen by 0.112 Å when the metal cation is Ni^+, while this lengthening[20] is only 0.087 Å when the metal cation is Cu^+. Similarly, the red-shifting of the corresponding stretching frequency, which upon Ni^+ association is, on average, 667 cm^{-1}, reduces to 447 cm^{-1} upon Cu^+ attachment.[20]

These dissimilarities are the direct consequence of more efficient donation and back-donation interactions when the reference acid is Ni^+. Actually, an inspection of the second-order orbital interaction energies indicates that donation from filled orbitals of the base into empty orbitals of the metal are more stabilizing for Ni^+ than for Cu^+. At the same time, the back-donation from the electron pairs of the metal to the antibonding orbitals of the base is also stronger for Ni^+ than for Cu^+. To understand these differences it must be taken into account that while Cu^+ is formally a closed-shell system, with all its d orbitals occupied, Ni^+ is an open-shell cation, with a vacancy in one of the d orbitals, and therefore it must behave as a better electron-acceptor. On the other hand, Cu^+, as a closed-shell system must be a poorer electron donor, as reflected in a higher

Table 3 Second-order interaction energies obtained in the NBO analysis. Orbital interaction energies are given in kJ mol^{-1}

	Electron-donor interaction	Back-donation		
Complex	Orbitals involved	Second-order Energy	Orbitals involved	Second-order Energy
S–C1	σ (C_1–H_7) → sd* (Ni)	61.5	n_d (Ni) → σ* (C_1–H_7)	17.9
	σ (C_3–H_6) → sd* (Ni)	61.5	n_d (Ni) → σ* (C_3–H_6)	17.9
S–Si4	σ (Si_3–H_5) → sd* (Ni)	133.7	n_d (Ni) → σ* (Si_3–H_5)	44.6
	σ (Si_3–H_6) → sd* (Ni)	133.3	n_d (Ni) → σ* (Si_3–H_6)	44.8
S–Ge4	σ (Ge_3–H_5) → sd* (Ni)	148.9	n_d (Ni) → σ* (Ge_3–H_5)	50.4
	σ (Ge_3–H_6) → sd* (Ni)	148.8	n_d (Ni) → σ* (Ge_3–H_6)	50.1
U–C1	π (C_1–C_2) → sd* (Ni)	278.1	n_d (Ni) → π* (C_1–C_2)	167.7
U–Si1	π (C_1–C_2) → sd* (Ni)	265.9	n_d (Ni) → π* (C_1–C_2)	175.4
U–Si2	σ (Si_3–H_5) → sd* (Ni)	113.5	n_d (Ni) → σ* (Si_3–H_5)	33.3
	σ (Si_3–H_6) → sd* (Ni)	113.5	n_d (Ni) → σ* (Si_3–H_6)	33.3
U–Si3	π (C_1–C_2) → sd* (Ni)	191.4	n_d (Ni) → π* (C_1–C_2)	128.0
	σ (Si_3–H_6) → sd* (Ni)	162.9	n_d (Ni) → σ* (Si_3–H_6)	19.7
U–Ge1	π (C_1–C_2) → sd* (Ni)	279.5	n_d (Ni) → π* (C_1–C_2)	157.9
U–Ge2	σ (Ge_3–H_5) → sd* (Ni)	150.5	n_d (Ni) → σ* (Ge_3–H_5)	52.7
	σ (Ge_3–H_6) → sd* (Ni)	150.5	n_d (Ni) → σ* (Ge_3–H_6)	52.7
U–Ge3	π (C_1–C_2) → sd* (Ni)	188.5	n_d (Ni) → π* (C_1–C_2)	127.5
	σ (Ge_3–H_6) → sd* (Ni)	171.6	n_d (Ni) → σ* (Ge_3–H_6)	23.2

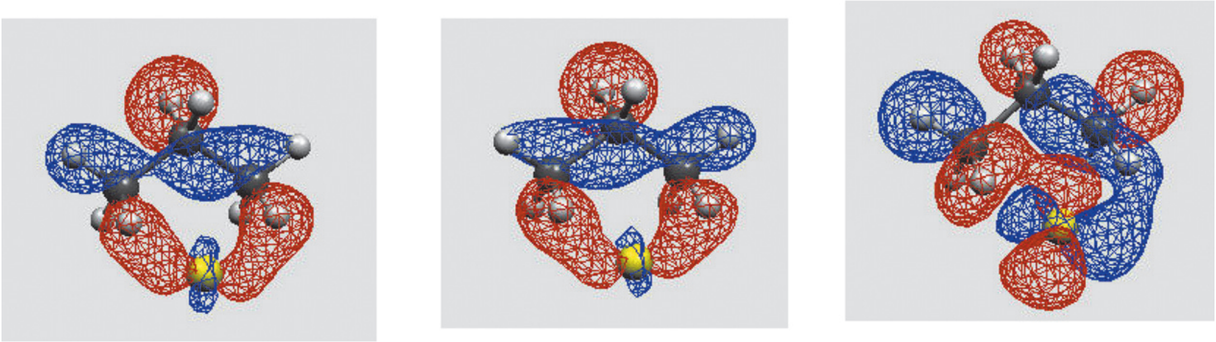

Fig. 3 Occupied molecular orbitals of propane–Ni^+ complexes, showing the three-centered bonding interaction between the d orbitals of the metal and the 1s orbitals of the hydrogen atoms of the terminal CH_3 groups.

ionization potential, and its n_d electron pair should be less diffuse than that of Ni^+.

These differences have also an important effect as far as the binding energies are concerned, in the sense that while propene behaves as a base slightly stronger than vinylsilane and vinylgermane towards Cu^+, the Si and Ge derivatives, both saturated and unsaturated, bind Ni^+ more strongly than propane and propene, respectively.

Conclusions

The interactions between H_3C–CH_2–XH_3 and H_2C=C(H)XH_3 (X = C, Si, Ge) compounds and Ni^+ in the gas phase involve agostic-type interactions between the metal and the hydrogen atoms of the XH_3 group. Only for propene is the conventional π-complex the global minimum of the PES. These agostic-type linkages can be viewed as three-center bonds resulting from electron donor interactions between σ_{XH} or π_{CC} bonding orbitals of the neutral and empty sd hybrid orbitals of the metal and back-donation from the electron pairs of the metal into the corresponding σ^*_{XH} or π^*_{CC} antibonding orbitals of the neutral. As a consequence, they are particularly stable for Si- and Ge-containing compounds, because of the high electron-donor ability of the XH_3 group to which the metal binds, when the heteroatom is Si or Ge. Consequently, ethylsilane and ethylgermane are predicted to bind Ni^+ much more strongly than propane. Vinylsilane and vinylgermane lead to non-conventional complexes in which the metal bridges the C_α atom of the C=C double bond and one of the hydrogen atoms of the XH_3 group, while propene yields a conventional π-complex as the most stable structure. In contrast with the behavior predicted when the reference acid is Cu^+, Si and Ge derivatives, both saturated and unsaturated, bind Ni^+ more strongly than propane and propene, respectively.

A comparison between Cu^+ and Ni^+ binding energies reveals that the latter are systematically greater than the former. One of the most important consequences of the greater strength of the interactions with Ni^+ is that the bond activation effects observed upon Ni^+ attachment are sizably larger than those found upon Cu^+ association.

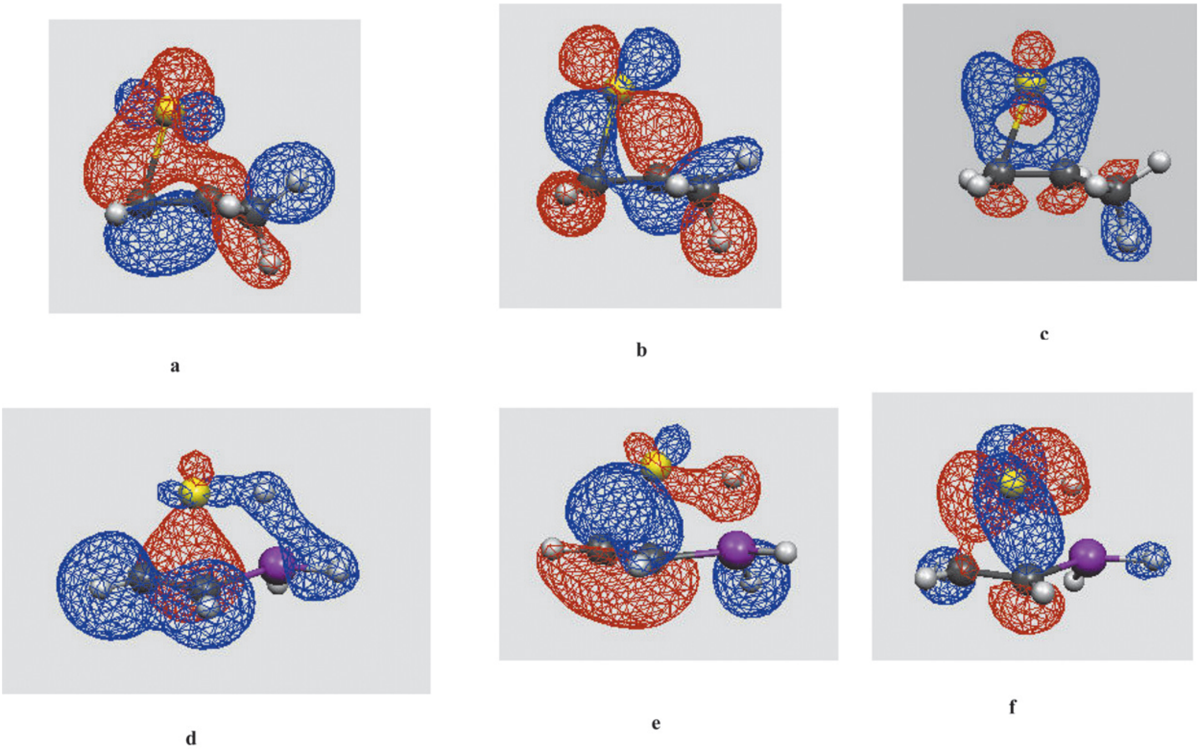

a

b

c

d

e

f

Fig. 4 Occupied molecular orbitals of propene–Ni^+ and vinylsilane–Ni^+ complexes. It can be seen that while in the former (orbitals a, b and c) the bonding interaction involves the d orbitals of the metal and the π-system of the neutral, for the latter the orbitals (d, e and f) are three-centered bonding combinations involving also the 1s orbital of one hydrogen of the SiH_3 group.

Acknowledgements

This work has been partially supported by the DGI Project No. BQU2000-0245. A generous allocation of computational time at the CCC of the Universidad Autónoma de Madrid is also acknowledged. I. C. gratefully acknowledges a FPU grant from the Ministerio de Educación, Cultura y Deporte of Spain.

References

1 T. G. Spiro, *Metal Ions in Biology*, Wiley, New York, 1980, vol. 1.
2 A. Fontijn, *Gas-Phase Metal Reactions*, North Holland, Amsterdam, 1992.
3 *Metal Ions in Biological Systems: Interactions of Metal Ions with Nucleotides, Nucleic Acids and their Constituents*, eds. A. Sigel and H. Sigel, Marcel Dekker, New York, 1996.
4 *Metal Ions in Biological Systems: Nickel and its Role in Biology*, eds. A. Sigel and H. Sigel, Marcel Dekker, New York, 1988.
5 P. E. M. Siegbahn and R. A. Blomberg, *Chem. Rev.*, 2000, **100**, 421.
6 S. H. Niu and M. B. Hall, *Chem. Rev.*, 2000, **100**, 353.
7 M. Torrent, M. Solà and G. Frenking, *Chem. Rev.*, 2000, **100**, 439.
8 F. Maseras, A. LLedós, E. Clot and O. Eisenstein, *Chem. Rev.*, 2000, **100**, 601.
9 H. Schwarz and D. Schroeder, *Pure Appl. Chem.*, 2000, **72**, 2319.
10 P. B. Armentrout, *Ann. Rev. Phys. Chem.*, 2001, **52**, 423.
11 B. S. Freiser, *Organometallic Ion Chemistry*, Kluwer Academic Publishers, Amsterdam, 1996.
12 O. Mó, M. Yáñez, M. Decouzon, J.-F. Gal, P.-C. Maria and J.-C. Guillemin, *J. Am. Chem. Soc.*, 1999, **121**, 4653.
13 J. L. M. Abboud, I. Alkorta, J. Z. Davalos, J. F. Gal, M. Herreros, P. C. Maria, O. Mó, M. T. Molina, R. Notario and M. Yáñez, *J. Am. Chem. Soc.*, 2000, **122**, 4451.
14 A. I. González, O. Mó and M. Yáñez, *J. Chem. Phys.*, 2000, **112**, 2258.
15 L. González, O. Mó, M. Yáñez, in *Recent Theoretical and Experimental Advances in Hydrogen Bonded Clusters*, ed. S. S. Xantheas, Kluwer Academic Publishers, Dordrecht, 2000, p. 393.
16 M. Lamsabhi, M. Alcamí, O. Mó, W. Bouab, M. Esseffar, J. L. M. Abboud and M. Yáñez, *J. Phys. Chem. A*, 2000, **104**, 5122.
17 A. Luna, M. Alcamí, O. Mó and M. Yáñez, *Int. J. Mass Spectrom. Ion Processes*, 2000, **201**, 215.
18 J.-F. Gal, M. Decouzon, P.-C. Maria, A. I. González, O. Mó, M. Yáñez, S. El Chaouch and J.-C. Guillemin, *J. Am. Chem. Soc.*, 2001, **123**, 6353.
19 I. Corral, O. Mó and M. Yáñez, *J. Comput. Methods Sci. Eng.*, 2002, **2**, 411.
20 I. Corral, O. Mó and M. Yáñez, *Int. J. Mass Spectrom. Ion Processes*, 2003, **227**, 401.
21 L. Galiano, M. Alcamí, O. Mó and M. Yáñez, *J. Phys. Chem. A*, 2002, **106**, 9306.
22 L. Galiano, M. Alcamí, O. Mó and M. Yáñez, *Chem. Phys. Chem.*, 2003, **4**, 72.
23 O. Mó, M. Yáñez, J.-F. Gal, P.-C. Maria and J.-C. Guillemin, *J. Phys. Org. Chem.*, 2002, **15**, 509.
24 I. Corral, O. Mó and M. Yáñez, *J. Phys. Chem. A*, 2003, **107**, 1370.
25 J.-C. Guillemin, L. Lassalle and T. Janati, *Planet. Space Sci.*, 1995, **43**, 75.
26 A. Chrostowska, V. Métail, G. Pfister-Guillouzo and J.-C. Guillemin, *J. Organomet. Chem.*, 1998, **570**, 175.
27 A. Luna, B. Amekraz, J. P. Morizur, J. Tortajada, O. Mó and M. Yáñez, *J. Phys. Chem. A*, 1997, **101**, 5931.
28 A. Luna, B. Amekraz, J. Tortajada, J. P. Morizur, M. Alcamí, O. Mó and M. Yáñez, *J. Am. Chem. Soc.*, 1998, **120**, 5411.
29 M. Alcamí, O. Mó, M. Yáñez, A. Luna, J. P. Morizur and J. Tortajada, *J. Phys. Chem. A*, 1998, **102**, 10 120.
30 A. Luna, B. Amekraz, J. P. Morizur, J. Tortajada, O. Mó and M. Yáñez, *J. Phys. Chem. A*, 2000, **104**, 3132.
31 A. Luna, M. Alcamí, O. Mó and M. Yáñez, *Chem. Phys. Lett.*, 2000, **320**, 129.
32 S. J. Klippenstein and C.-N. Yang, *Int. J. Mass Spectrom. Ion Processes*, 2000, **201**, 253.
33 M. Alcamí, O. Mó and M. Yáñez, *Mass Spectrom. Rev.*, 2001, **20**, 195.
34 T. K. Ghanty and E. R. Davidson, *Int. J. Quantum Chem.*, 2000, **77**, 291.
35 M. J. Frisch, G. W. Trucks, H. B. Schlegel, G. E. Scuseria, M. A. Robb, J. R. Cheeseman, V. G. Zakrzewski, J. J. A. Montgomery, R. E. Stratmann, J. C. Burant, S. Dapprich, J. M. Millam, A. D. Daniels, K. N. Kudin, M. C. Strain, O. Farkas, J. Tomasi, V. Barone, M. Cossi, R. Cammi, B. Mennucci, C. Pomelli, C. Adamo, S. Clifford, J. Ochterski, G. A. Petersson, P. Y. Ayala, Q. Cui, K. Morokuma, D. K. Malick, A. D. Rabuck, K. Raghavachari, J. B. Foresman, J. Cioslowski, J. V. Ortiz, B. B. Stefanov, G. Liu, A. Liashenko, P. Piskorz, I. Komaromi, R. Gomperts, R. L. Martin, D. J. Fox, T. Keith, M. A. Al-Laham, C. Y. Peng, A. Nanayakkara, C. González;, M. Challacombe, P. M. W. Gill, B. Johnson, W. Chen, M. W. Wong, J. L. Andres, C. González, M. Head-Gordon, E. S. Replogle and J. A. Pople, *GAUSSIAN 98 (Revision A.3)*, Gaussian, Inc., Pittsburgh, PA, 1999.
36 A. D. Becke, *Phys. Rev. A*, 1988, **38**, 3098.
37 C. Lee, W. Yang and R. G. Parr, *Phys. Rev. B*, 1988, **37**, 785.
38 A. J. H. Wachters, *J. Chem. Phys.*, 1970, **52**, 1033.
39 P. J. Hay, *J. Chem. Phys.*, 1977, **66**, 4377.
40 A. P. Scott and L. Radom, *J. Phys. Chem.*, 1996, **100**, 16 502.
41 R. Georgiadis, E. R. Fisher and P. B. Armentrout, *J. Am. Chem. Soc.*, 1989, **111**, 4251.
42 C. W. Bauschlicher, S. R. Langhoff, H. Partridge and L. A. Barnes, *J. Chem. Phys.*, 1989, **87**, 2399.
43 R. F. W. Bader, *Atoms in Molecules. A Quantum Theory*, Clarendon Press, Oxford, 1990.
44 A. E. Reed, L. A. Curtiss and F. Weinhold, *Chem. Rev.*, 1988, **88**, 899.
45 J. K. Perry, G. Ohanessian and W. A. Goddard III, *J. Phys. Chem.*, 1993, **97**, 5238.
46 P. L. A. Popelier and G. Logothetis, *J. Organomet. Chem.*, 1998, **555**, 101.
47 M. Brookhart and M. L. H. Green, *J. Organomet. Chem.*, 1983, **250**, 395.
48 M. D. Butts, J. C. Bryan, X.-L. Luo and G. Kubas, *Inorg. Chem.*, 1997, **36**, 3341.
49 G. I. Nikonov, P. Mountford, S. K. Ignatov, J. C. Green, M. A. Leech, G. L. Kuzmina, A. G. Razuvaev, N. H. Rees, A. J. Blake, J. A. K. Howard and D. A. Lemenovskii, *J. Chem. Soc., Dalton Trans.*, 2001, 2903.
50 S. Trofimenko, *J. Am. Chem. Soc.*, 1967, **89**, 6288.
51 S. Trofimenko, *J. Am. Chem. Soc.*, 1968, **90**, 4754.
52 F. A. Cotton, T. LaCour and A. G. Stanislowski, *J. Am. Chem. Soc.*, 1974, **96**, 754.
53 J. W. M. Carneiro, P. v. R. Schleyer, M. Saunders, R. Remington, H. F. Schaefer III, A. Rauk and T. S. Sorensen, *J. Am. Chem. Soc.*, 1994, **116**, 3483.
54 A. L. L. East, Z. F. Liu, C. McCague, K. Cheng and J. S. Tse, *J. Phys. Chem. A*, 1998, **102**, 10 903.
55 M. N. Glukhovtsev and R. D. Bach, *Chem. Phys. Lett.*, 1998, **286**, 51.
56 S. J. Collins and P. J. O'Malley, *J. Chem. Soc., Faraday Trans.*, 1996, **92**, 4347.
57 J. L. M. Abboud, M. Herreros, R. Notario, M. Esseffar, O. Mó and M. Yáñez, *J. Am. Chem. Soc.*, 1996, **118**, 1126.